Taken altogether, the recovery of Cx32 expression could be proposed to have an effect on enhancing the liver-specific functions in hepatoma cells, in addition to improving the biological safety of hepatoma cells for the application as tissue engineered artificial liver by the inhibition of malignant growth of tumor cells of HepG2.

In conclusion, this study is the first to report a clear increase in the functional GJIC in HepG2 by transfection of Cx32 gene, and the subsequently enhanced liver-specific functions of ammonia detoxification and albumin synthesis in the Cx32 gene transfected HepG2. It may be expected to improve cellular functions of the hepatoma cell line by Cx32 gene transfection and serve to develop an excellent biohybrid-artificial liver.

Acknowledgments

We are grateful to the support of Japan Society for the Promotion of Science, and Health and Labour Sciences Research Grants, Research on Advanced Medical Technology, Ministry of Health, Labour and Welfare and Japan Health Sciences Foundation.

References

[1] N.M. Kumar, N.B. Gilula, The gap junction communication channel, Cell 84 (1996) 381–388.
[2] A. Ito, F. Katoh, T.R. Kataoka, M. Okada, N. Tsubota, H. Asada, K. Yoshikawa, S. Maeda, Y. Kitamura, H. Yamasaki, H. Nojima, A role for heterologous gap junctions between melanoma and endothelial cells in metastasis, J. Clin. Invest. 105 (2000) 1189–1197.
[3] H. Yamasaki, V. Krutovskikh, M. Mesnil, T. Tanaka, M.L. Zaidan-Dagli, Y. Omori, Role of connexin (gap junction) genes in cell growth control and carcinogenesis, C.R. Acad. Sci. Paris, Sciences de la vie/Life Sciences 322 (1999) 151–159.
[4] R. Bruzzone, T.W. White, D.L. Paul, Connections with connexins: the molecular basis of direct intercellular signaling, Eur. J. Biochem. 238 (1996) 1–27.
[5] D.A. Goodenough, J.A. Goliger, D.L. Paul, Connexins, connexons and intercellular communication, Annu. Rev. Biochem. 65 (1996) 475–502.
[6] D.C. Spray, J.C. Saez, E.L. Hertzberg, R. Dermietzel, Gap junctions in liver, composition, function, and regulation, in: I.M. Arias, J.L. Boyer, N. Fausto, W.B. Jacoby, D.A. Schachter, D.A. Shafritz (Eds.), The Liver Biology and Pathobiology, third ed., Raven, New York, 1994, pp. 951–967.
[7] D.L. Paul, Molecular cloning of cDNA for rat liver gap junction protein, J. Cell Biol. 103 (1986) 123–134.
[8] E. Eghbali, J.A. Kessler, L.M. Reid, C. Roy, D.C. Spray, Involvement of gap junctions in tumorigenesis: transfection of tumor cells with connexin 32 cDNA retards growth in vivo, Proc. Natl. Acad. Sci. USA 88 (1991) 10701–10705.
[9] M. Evert, T. Ott, A. Temme, K. Willecke, F. Dombrowski, Morphology and morphometric investigation of hepatocellular preneoplastic lesions and neoplasms in connexin32-deficient mice, Carcinogenesis 23 (2002) 697–703.
[10] N.L. Sussman, G.T. Gislason, C.A. Conlin, J.H. Kelly, The hepatix extracorporeal liver assist device-initial clinical experience, Artif. Organs 18 (1994) 390–396.
[11] Y. Yamashita, M. Shimada, E. Tsujita, S. Tanaka, H. Ijima, K. Nakazawa, R. Sakiyama, J. Fukuda, T. Ueda, K. Funatsu, K. Sugimachi, Polyurethane foam/spheroid culture system using human hepatoblastoma cell line (HepG2) as a possible new hybrid artificial liver, Cell Transpl. 10 (2001) 717–722.
[12] M. Takagi, N. Fukuda, T. Yoshida, Comparison of different hepatocyte cell lines for use in a hybrid artificial liver model, Cytotechnology 24 (1997) 39–45.
[13] M.H. El-Fouly, J.E. Trosko, C.C. Chang, Scrape-loading and transfer: a rapid and simple technique to study gap junctional intercellular communication, Exp. Cell Res. 168 (1987) 422–430.
[14] H. Yamasaki, V. Krutovskikh, M. Mesnil, T. Tanaka, M.L. Zaidan-Dagli, Y. Omori, Role of connexin (gap junction) genes in cell growth control and carcinogenesis, C.R. Acad. Sci. III 3222 (1999) 151–159.
[15] Y. Omori, V. Krutovskikh, N. Mironov, H. Tsuda, H. Yamasaki, Cx32 gene mutation in a chemically induced rat liver tumour, Carcinogenesis 17 (1996) 2077–2080.
[16] P.E.M. Martin, G. Blundell, S. Ahmad, R.J. Errington, W.H. Evans, Multiple pathways in the trafficking and assembly of connexin 26, 32 and 43 into gap junction intercellular communication channels, J. Cell Sci. 114 (2001) 3845–3855.
[17] T. Kojima, D.C. Spray, Y. Kokai, H. Chiba, Y. Mochizuki, N. Sawada, Cx32 formation and/or Cx32-mediated intercellular communication induces expression and function of tight junctions in hepatocytic cell line, Exp. Cell Res. 276 (2002) 40–51.
[18] R.G. Johnson, R.A. Meyer, X.R. Li, D.M. Preus, L. Tan, H. Grunenwald, A.F. Paulson, D.W. Laird, J.D. Sheridan, Gap junctions assemble in the presence of cytoskeletal inhibitors, but enhanced assembly requires microtubules, Exp. Cell Res. 275 (2002) 67–80.
[19] G. Cairo, M. Lucchini, Molecular basis of reduced albumin gene expression in hepatoma cell lines with different growth rates, Exp. Cell Res. 206 (1993) 255–260.
[20] D. Haussinger, Nitrogen metabolism in liver: structural and functional organization and physiological relevance, Biochem. J. 267 (1990) 281–290.
[21] E. Rosenberg, R.A. Faris, D.C. Spray, B. Monfils, S. Abreu, I. Danishefsky, L.M. Reid, Correlation of expression of Connexin mRNA isoforms with degree of cellular differentiation, Cell Adhes. Commun. 4 (1996) 223–235.

季刊フラーレン Vol.11, No. 2, 2003 （通巻４１号）別刷

特別企画

単分子ナノマニピュレーションを目指した超化学分子とナノテクノロジーを用いた解析。機能性人工レセプター Molecular Gripper の設計合成及び画像化.

国立医薬品食品衛生研究所

山 越　葉 子

２００３年4月

発行：　株式会社 ダイヤリサーチマーテック

DIA RESEARCH MARTECH INC.

6．特別企画（第４２回）

単分子ナノマニピュレーションを目指した超分子化学とナノテクノロジーを用いた解析 －機能性人工レセプター Molecular Gripperの設計合成および画像化－[1]

国立医薬品食品衛生研究所　山越 葉子

新規機能性人工レセプター"Mecanoreceptor" を設計・合成し，機能性を分光学的手法およびナノテクノロジーにより解析した．本レセプターは，温度感受性の包接部分と，金表面に吸着するチオエーテル部分，およびリンカー部分としてのアルキル基を有する．これらのレセプターが金単結晶表面 (Au(111))に形成した自己組織化膜を走査型顕微鏡(STM)を用いた原子レベルでの解析に供した．

1. はじめに

1980 年代に IBM–Zürich 研究所のグループにより開発された走査型トンネル顕微鏡 (STM)[2]，原子間力顕微鏡 (AFM)[3] をはじめとする走査型プローブ顕微鏡 (SPM) の発展は，分子を単分子のレベルで観測したり操作することを可能にした．STM は探針と電導性サンプルとの間に生じるトンネル電流を，AFM は微細なカンチレバーと分子との原子間力を媒介とした測定法であり，最近では原子像の画像化[4] (Figure 1.) のみならず，原子レベルで微細なプローブを用いた単分子マニピュレーション[5] (Figure 2.) も可能になった．

他方超分子化学の分野では，分子間相互作用を利用した機能的分子マシーンや生体ミミックな構造体の構築を目的とした研究がなされているが，ナノテクノロジーがもつ技術力を用いるとさらに新規かつ複雑な構造体が得られる可能性がある．こういった複雑な構造体を構築する道具の第一歩として，本研究においては機能性人工レセプター "Mecanoreceptor" をデザインし，合成した．Mecanoreceptor の大きな特徴は，物理的あるいは化学的変化（温度，光，電圧，分子間力，pH，化学物質など）によりゲスト分子の内包あるいは放出をコントロールできる機能的リガンド結合部位があることである．

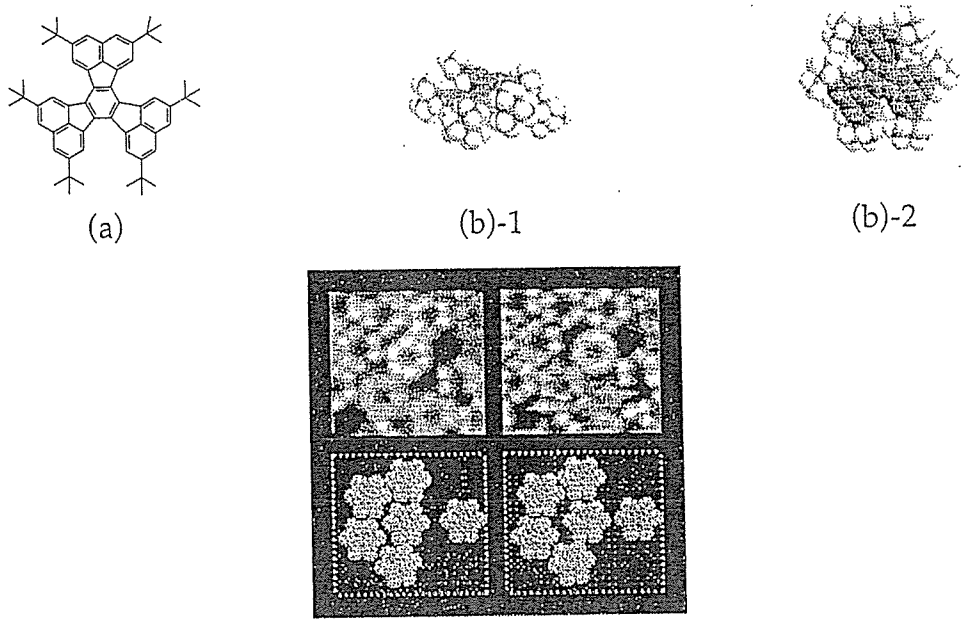

(a) (b)-1 (b)-2

(c)

Figure 1. 原子レベル解像度での有機分子の画像化の例.
Structure of molecular bearing (a), molecular model (b) and STM image (c) of molecular bearing.
(These pictures are kindly provided by Drs. Schelittler and Gimzewski in IBM.)

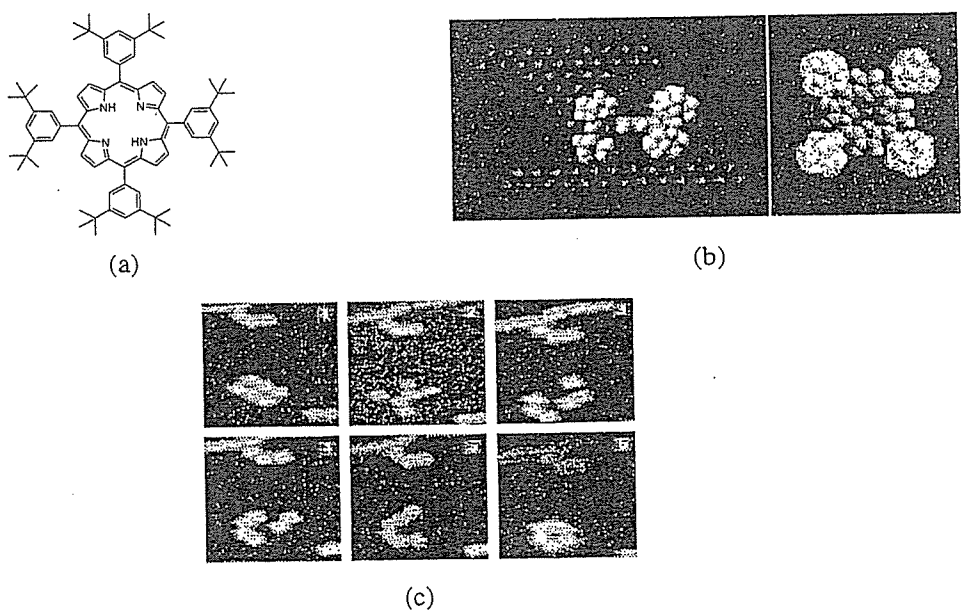

(a) (b)

(c)

Figure 2. STM 探針を用いた有機分子の探分子マニピュレーション.
(These pictures are kindly provided by Drs. Schelittler and Gimzewski in IBM.)

2. Mecanoreceptor のデザイン

我々がデザインした Mecanoreceptor は Figure 3. に示すように 3 つの部分：

（1）ホストーゲスト結合が温度変化により調整できるゲスト包接部分，（2）配向性を調整でき，包接部分のフレキシビリティーを保つスペーサーとなるリンカー部分，（3）金表面に結合できる官能基 からなる．本研究においては，特にゲスト部分に，Cram らが報告したフレキシブルキャビタンド[6] を用いることを計画した．このキャビタンドは Figure 4. に示すように，低温では表面積の大きい開いた形の Kite コンフォーメーションを，常温あるいは比較的高温では，内側にキャビティを有する閉じた形の Vase コンフォーメーションをとることが知られている．また，特に Vase コンフォーメーションにおいては特定のゲスト化合物の内包という機能性も有する．

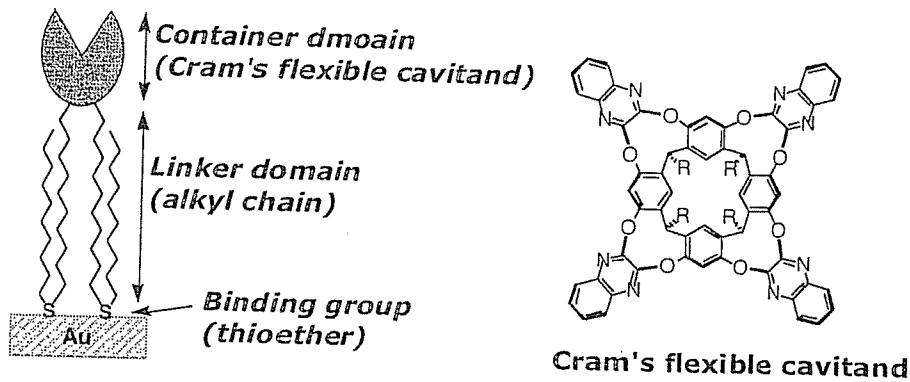

Figure 3. Mecanoreceptor の設計．

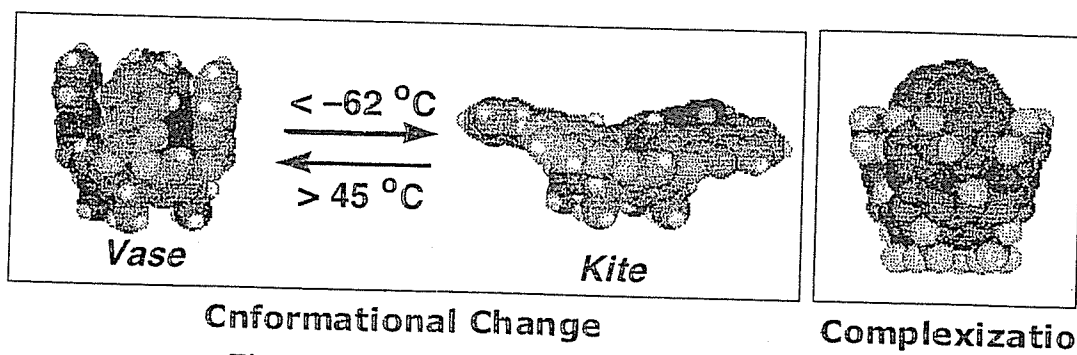

Figure 4. Cram のキャビタンドの機能性．
（温度変化に伴うコンフォーメーション変化．ゲスト分子内包性．
ゲスト分子としてはシミュレーションとして C_{60} を示した．）

我々がこの機能性キャビタンドを有する Mecanoreceptor を用いて目指した主な２つのアウトプットを Figure 5 および 6 に示す．まず，Figure 5. に示すように，こうした機能性レセプターは分子グリッパーとして利用できる可能性を有する．すなわち，ナノメートルオーダーで位置を調整できるピエゾ素子に結合させた SPM の探針の先端にこの Mecanoreceptor を結合させる．先端部のフレキシブルキャビタンドは温度を変化させることでゲスト分子の単分子レベ

ルでの包接および放出をコントロールできる．この特性を利用し，温度を低温から高温に移行させることで，ゲスト分子を選択的に認識，包接，保持し，ピエゾ素子の動きにより目的の位置にレセプターを移動させ，これを再び冷却することにより分子を放出し，表面上の思った位置に自在に配置することができる．

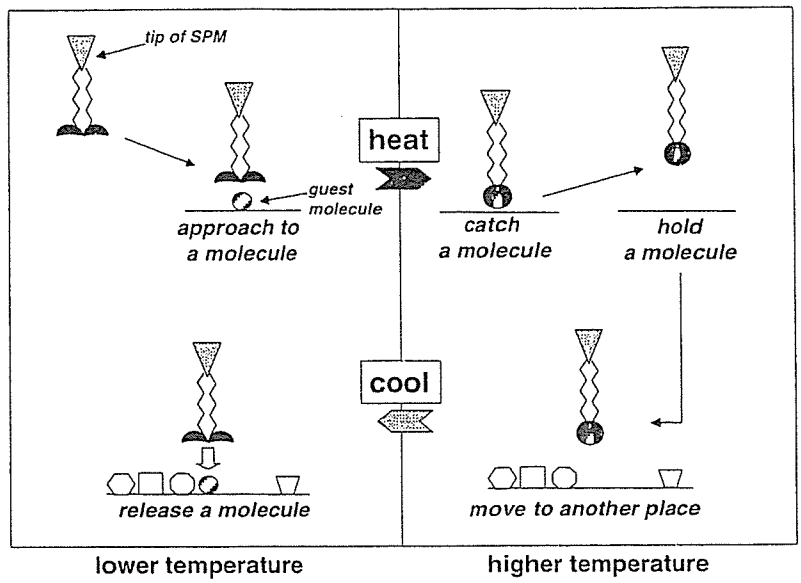

Figure 5. Mecanoreceptor のコンセプトⅠ．
(single molecule manipulation)

Mecanoreceptor の第二のアプリケーションとしては，Figure 6.に示すような機能性表面の構築が挙げられる．すなわち，レセプターのスィッチングによりゲスト化合物の放出がコントロールできる表面を構築し，必要に応じてゲスト化合物の機能発現を制御するというアイデアである．

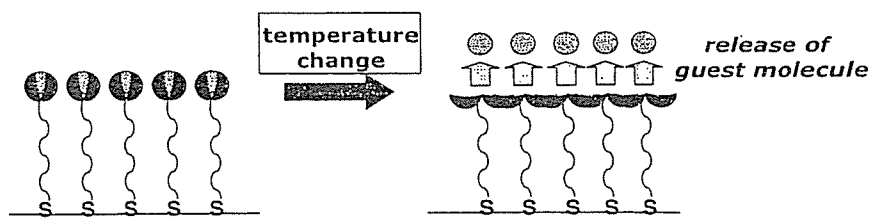

Figure 6. Mecanoreceptor のコンセプトⅡ．
(functional surface with controlled release of guest molecule)

3. 人工レセプターの合成

以上のコンセプトに基づき，第一世代の Mecanoreceptor の合成に取り組んだ．まず，レセプターが機能を発揮するかどうかを分光学的手法およびナノテ

クノロジーを用いて解析するため，金単分子表面上に自己組織化膜を形成する分子をデザインし，合成を行った．合成スキームを Figure 7, 8. に示す．

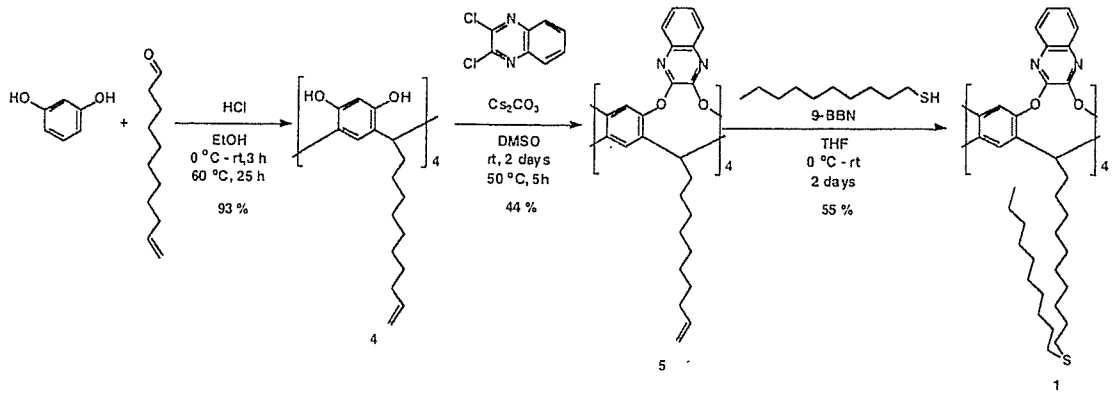

Figure 7. Synthesis of Mecanoreceptor A (1) with C_{10} thioether legs.

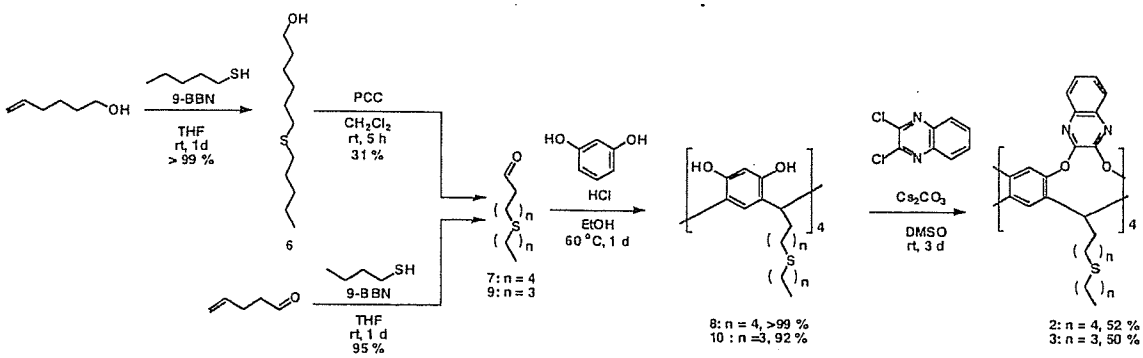

Figure 8. Synthesis of Mecanoreceptors B (3) and C (2) with C_5 and C_4 thioether legs, respectively.

キャビタンド部分の基本骨格をなすレゾルシナレン部分は，レゾルシノールと相当するアルデヒドとの酸触媒下縮合反応により効率良く合成された．レゾルシナレン骨格に炭酸セシウムをベースとして用いて，キノキサリン基を結合させることで，温度感受性キャビタンドを構築した．また，チオエーテル部分は，9-BBN を触媒とするラジカル付加により合成した．

4. 人工レセプターの分光学的解析

合成した Mecanoreceptor A を用いて温度可変 NMR を用いて溶液中におけるコンフォーメーション変化について解析した．結果を Figure 9. に示す．

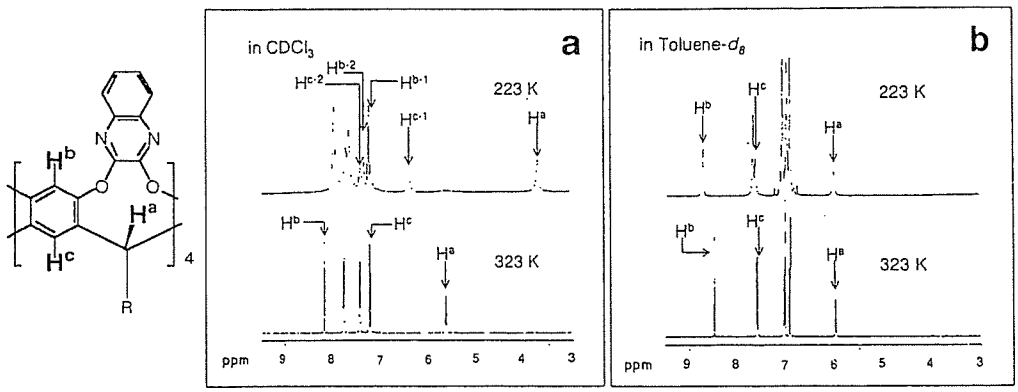

Figure 9. Selected NMR spectra from variable temperature studies. (a) measured in $CDCl_3$. (b) measured in toluene-d_8.

ここに示すように，重クロロホルム中では，常温下の測定結果に比較し，低温下では H^a プロトンのケミカルシフトが大きくシフトし，また，常温下では等価な 4 つの H^b および H^c プロトンが 2 種類に分かれている結果となり，Kite コンフォーメーションをとっていることが示唆された．他方，重トルエン中での測定結果によると，低温下での測定結果と常温下での測定結果に大きな違いはなく，温度によるコンフォーメーションの変化は見られなかった．これは，トルエン分子がゲスト化合物としてキャビタンド内に包接され，キャビタンド分子が Kite コンフォーメーションへと広がるのを妨げているためと推測された．

5. 機能性人工レセプターの STM による画像化

合成した三種の Mecanoreceptor を用い，溶液法に基づき自己組織化膜を形成し，表面解析に供した．すなわち，割りたてのフレッシュなマイカを基礎基盤として用い，高真空下（10^{-5} mbar 程度）350 – 380 °C にて 0.5 – 1 時間予熱後，同じ温度下で加熱しながら 2 nm / min の速さで 50 – 70 nm の厚さまで金を蒸着した．この金サブストレートは，大気中下の STM 測定により予備的に表面を解析し，約 2.46 Å の高さのステップを有する単結晶表面 (Au(111)) であることを確認した．自己組織化膜はおのおのの Mecanoreceptor の 1 mM クロロホルム溶液中に金サブストレートを浸漬し，常温下にて 16 時間インキュベートすることで調製した．Table I. に示す表面解析の結果により，いずれの Mecanoreceptor も自己組織化膜を形成していることが示された．

これらの自己組織化膜を高真空下 STM 解析に用いた．一般的に，トンネル電流を伴う解析法である STM 測定には，電導性あるいは半導性のサンプルが適しているため，C_{10} アルキル鎖を有する Mecanoreceptor A により形成される自己組織化膜は厚いため，低電流測定法が必要であると考えられ，それに対し，C_5 あるいは C_4 アルキル鎖を有する Mecanoreceptor B および C により形成される自己組織化膜のほうが，比較的容易に測定が可能であると思われた．しかし，

それぞれを測定に用いた結果，Mecanoreceptor B, C による自己組織化膜は測定に対し安定ではなく，走査した探針により分子が基盤からはがれてしまった．これは，安定な自己組織化膜を形成するのに十分な長さのアルキル基を有していなかったためと考えられる (Figure 10.)．それに対し，最も安定な自己組織化膜を形成した Mecanoreceptor A は原子像の画像化に成功した．結果を Figure 11. に示す．図に示したように，Mecanoreceptor のキャビタンド部分は，閉じられた Vase 型のコンフォーメーションをとりながら自己組織化膜を形成していることが示された．

Table I. Monolayer characterization by ellipsometry and contact angle measurement.

Compounds	Calculated thickness[b]	Contact angle (H_2O)[a]	
		θ_a/°	θ_r/°
A	1.56	97±6	85±3
B	1.13	90±1	57±1
C	0.94	93±2	63±2

[a] θ_a and θ_r are advancing and receding contact angles, respectively.
[b] Calculated from ellipsometric data.

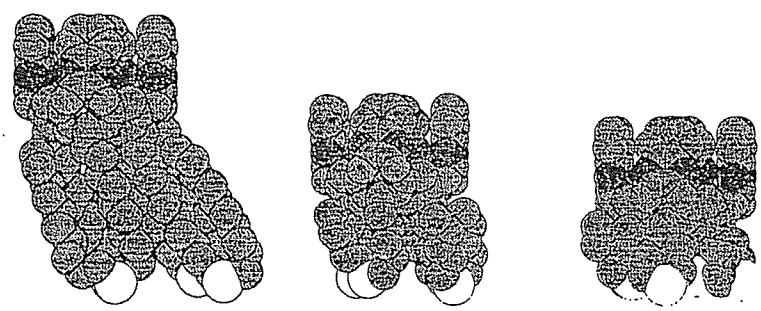

(a) (b) (c)

Figure 10. CPK models (side views) of three mecanoreceptors A (a), B (b) and C (c) with different lengthes of dialkylthioether legs (calculated by amber* force field program operated by Macromodel Ver. 7.0).

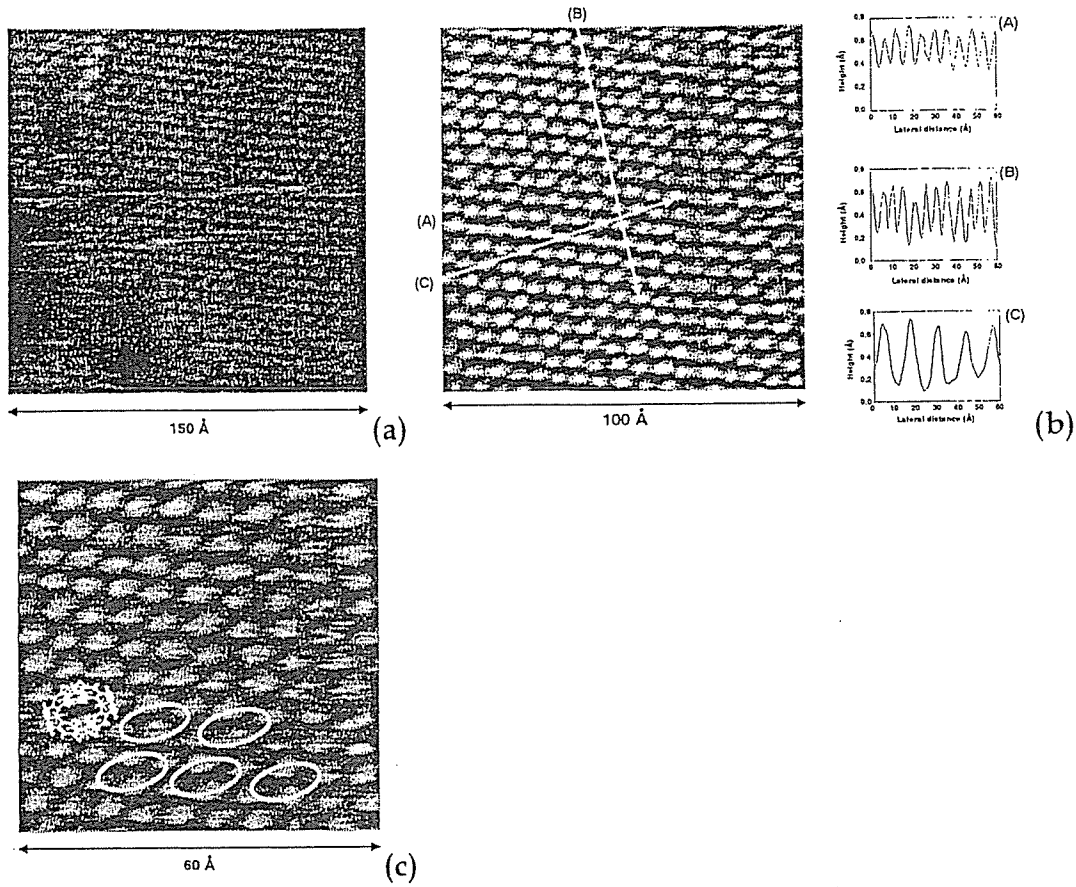

Figure 11. STM Images of SAM of Mecanoreceptor A absorbed on Au(111). The images were taken in contrast mode with I_t = 1.63 pA and V_t = 2.0 V for (a) and (b) and V_t = 1.9 V for (c).

(a) Image of monolayer with grain boundaries.

(b) Image of well-packed region and its cross sections. Distances of between bright spots are *ca.* 0.6 nm in cross sections (A) and (B) and *ca.* 1.1 nm in cross section (C).

(c) Image with the drawing of a structural model for the cavitand. The ellipses outline individual molecule of A.

6. おわりに

三種の異なるアルキル基を有する Mecanoreceptoe A - C を合成し，溶液中で温度依存的なコンフォーメーション変化が起きることを確認した．更にこれを用いて自己組織化膜を調製し，最も安定な膜を形成した Mecanoreceptor A に関して超高真空型 STM を用いた原子像解析に成功した．今後，これを Molecular Gripper として発展させるべく，低温下 STM 測定および足場部分の改良などが期待される．

本研究はスイス連邦工科大学 (ETH-Zürich) の François Diederich 教授と

Studies on the tumor promoting mechanism of hard and soft segment models of polyetherurethane: Tyr^{265} phosphorylation of connexin43 is a key step in the GJIC inhibitory reaction induced by polyetherurethane

Akira Ichikawa,[1,2] Toshie Tsuchiya[1]
[1]*Division of Medical Devices, National Institute of Health Sciences, 1-18-1 Kamiyoga, Setagaya-ku, Tokyo 158-8501, Japan*
[2]*Domestic Research Fellow, Japan Science and Technology Corporation, 4-1-8 Honcho, Kawaguchi 332-0012, Japan*

Received 5 October 2001; revised 2 January 2002; accepted 17 January 2002
Published online 9 July 2002 in Wiley InterScience (www.interscience.wiley.com). DOI: 10.1002/jbm.10239

Abstract: Gap junctional intercellular communication (GJIC) is inhibited by 4,4′-di(ethoxycarboamide) diphenylmethane (MDU) and polytetramethylene oxide 1000 (PTMO1000), which are model chemicals of hard and soft segments of polyetherurethane (PEU), respectively. In our previous study, we suggested that the inhibition of GJIC induced by MDU and PTMO1000 may lead to accelerate promotion step by both segments after the initiation step by hard segment, MDU. To examine this hypothesis, we established connexin 43 overexpressed clones from Balb/c 3T3 A31-1-1 clones (A31-1-1 cells) by transfection. Here we show that these clones acquired much higher GJIC ability than parental A31-1-1 cells and kept them even if MDU or PTMO1000 was added to the culture. We also found that Mutation of Cx43 at Tyr-265 resulted in reduced inhibition of GJIC induced by MDU and PTMO1000. These findings suggest that inhibition of GJIC by PEU may be caused by Tyr-265 phosphorylation of Cx43 molecule. © 2002 Wiley Periodicals, Inc. J Biomed Mater Res 62: 157–162, 2002

Key words: Balb/c 3T3 A31-1-1 cells; connexin 43; gap junctional intercellular communication; polyetherurethane; tyrosine phosphorylation

INTRODUCTION

Gap junctions are structures in the plasma membranes of most animal cell types that form aqueous channels interconnecting the cytoplasms of adjacent cells.[1,2] Gap junctions permit the intercellular passage of small molecules and have been implicated in diverse biological processes, such as development, differentiation, cellular metabolism, and cellular growth control. Gap junctions are composed of six connexin molecules, which are a conserved family of proteins with four membrane-spanning regions and with cytoplasmic amino- and carboxy-terminus. Gap junctions are known to be regulated by posttranslational phosphorylation of the carboxy-terminal tail region on connexin molecule. Phosphorylation has been implicated in the regulation of a broad variety of connexin processes, such as the trafficking, assembly/disassembly, degradation, as well as the gating of gap junction channels.

Correspondence to: T. Tsuchiya; e-mail: tsuchiya@nihs.go.jp

Polyetherurethanes (PEUs) are used for implant applications because of their useful elastomeric properties and their high tensile strength, lubricity, good abrasion resistance, and ease of handling. However, some kinds of PEUs are known to be unstable in body,[3,4] and induced tumors in rats.[5] We have reported the tumorigenic potentials of these PEUs *in vivo* and *in vitro*.[6,7] PEU-components had inhibited gap junctional intercellular communication (GJIC) in cultures of Balb/c 3T3 A31-1-1 cells and Chinese hamster V79 fibroblasts.[8–10]

In this study, we established Cx43-overexpressing Balb/c 3T3 A31-1-1 cells and evaluated for GJIC activities under the existence of MDU and PTMO1000, which are hard and soft segments of PEUs, respectively. Furthermore, we constructed the tyrosine 265 to phenylalanine substitution (Y265F) mutant of Cx43 and compared the effect on GJIC activities with wild-type Cx43 transfectant.

MATERIALS AND METHODS

Chemicals

4,4′-Di(ethoxycarboamide) diphenylmethane (MDU) synthesized in our laboratory was used as a hard segment

model chemical of PEU. Polytetramethylene oxide 1000 (PTMO1000) was used as a monomer consists of soft segment of PEU. Chemical structures are showed in Figure 1.

Cells and cell culture

Balb/c 3T3 A31-1-1 cells and its transfectant clones were cultured in minimal essential medium (MEM) containing 10% fetal bovine serum (FBS). Cell cultures were maintained in a 37°C incubator under a humidified 5% CO_2 atmosphere and were routinely subcultured by trypsinization.

Site-directed mutagenesis and plasmid construction

A full-length Cx43 DNA fragment was amplified by polymerase chain reaction (PCR) using primers Cx43F (5'-TTGACTCGAGCCTCCAAGGAGTTCCACCAACT-3') and Cx43R (5'-CAACTCGAGTTAAATCTCCAGGTCATCAGGCC-3'). The *Xho*I site (CTCGAG, underlined) was inserted into these primers for subcloning into a mammalian expression vector pB45-neo.[11] The cloned 1217-bp PCR fragment was subcloned into pB45-neo. The mutant form of Cx43 was prepared from the full-length Cx43 DNA fragment using the splicing by overlap extension (SOE) method with primers Cx43Y265F-sense (5'-GATCTCCAAAATTCGCCTACTTCAA-3') and Cx43Y265F-antisense (5'-TTGAAGTAGGCGAATTTTGGAGATC-3') designed to alter a tyrosine residue to phenylalanine. The fidelity of the mutant was confirmed by sequencing the full-length Cx43 DNA.

Transfection

The Cx43 expression vector pB45-Cx43-neo and the control vector pB45-neo were then transfected into Balb/c 3T3 A31-1-1 cells using the SuperFect reagent (QIAGEN K.K., Tokyo, Japan) according to manufacturer's instruction. Stable transfectant clones were selected with 500 μg/mL G418 (Life Technologies, Inc., Frederick, MD), and clones were isolated using cylinder trypsinization method followed by further expansion and storage at −85°C.

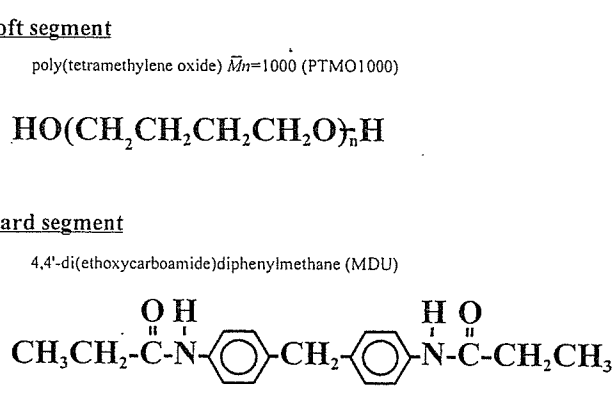

Figure 1. Chemical structure of segmented polyetherurethane.

Western blot

When cells reached confluence in 60-mm tissue culture dishes, all cells were lysed directly in 500 μL of lysis buffer [50 m*M* Tris-HCl, pH 6.8, 2% sodium dodecyl sulfate (SDS), 1 m*M* phenylmethylsulfonyl fluoride]. Protein concentrations of lysates were measured using D/C protein assay kit (Bio-Rad Laboratories, Hercules, CA) according to manufacturer's instruction. Equal amounts of proteins dissolved in gel loading buffer (50 m*M* Tris-HCl, pH 6.8, 100 m*M* 2-mercaptoethanol, 2% SDS, 0.1% bromophenol blue, 10% glycerol) were analyzed by 7.5% SDS-polyacrylamide gel electrophoresis, and proteins were transferred to Hybond-ECL nitrocellulose membranes (Amersham Pharmacia Biotech UK Limited, Buckinghamshire, UK). Cx43 protein was detected by anti-Cx43 polyclonal antibodies (Zymed Laboratories, Inc., San Francisco, CA) and ECL system (Amersham Pharmacia Biotech UK Limited). Phosphorylation levels of Cx43 were quantified by densitometry.

Scrape-loading and dye transfer assay for detection of GJIC

The scrape-loading and dye transfer (SLDT) technique was adapted after the method of El-Fouly et al.[12] Confluent monolayer cells in 35-mm culture dishes were used. MDU and PTMO1000 dissolved in dimethylsulfoxide (DMSO) were added to the culture medium and incubated for 24 h. After rinsing with Ca^{2+} Mg^{2+} phosphate-buffered saline [PBS (+)], cell dishes were loaded with 0.05% Lucifer Yellow (Molecular Probes, Eugene, OR)/PBS (+) solution and were scraped immediately with a sharp blade. After incubation for 5 min at 37°C, cells were washed with PBS (+) and monitored using fluorescence microscope. The distance the dye migrated was measured from the cell layer at the scrape to the edge of the dye front that was visually detectable.[13]

RESULTS

Establishment of Cx43 over-expressed A31-1-1 cells

A31-1-1 cells were transfected with a full-length rat Cx43 cDNA. Colonies resistant to G418 were isolated with cylinder trypsinization method and screened by Western blot analysis. Wild-type (A31-1-1/Cx43) and mutant Cx43 (A31-1-1/Cx43Y265F) transfected clones showed high level of Cx43 protein expression [Fig. 2(A)]. In order to eliminate possible effects of vector plasmid DNA on GJIC characteristics and Cx43 expression level of transfectant clones, A31-1-1 cells

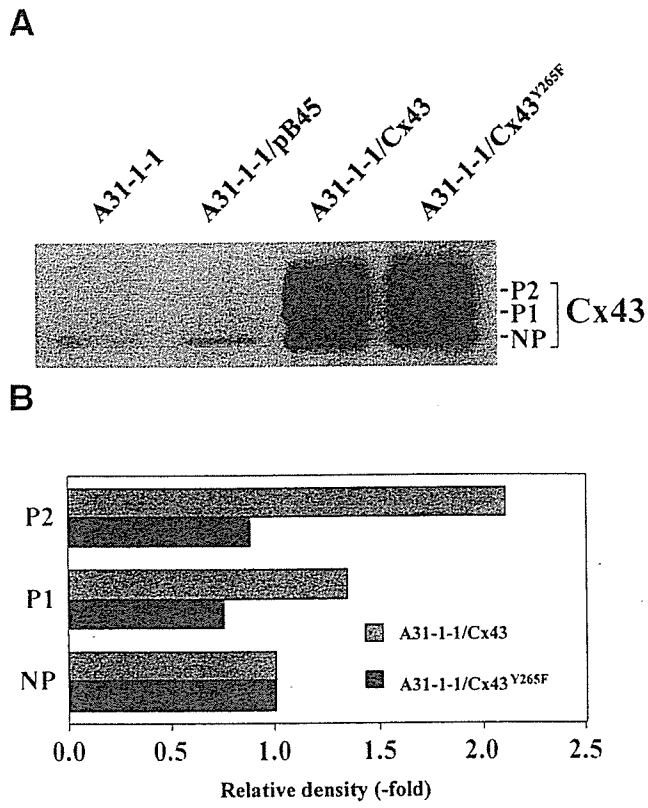

Figure 2. Establishment of Cx43 and Cx43Y265F overexpressed A31-1-1 cells. (A) Western blot of the control A31-1-1 cells and transfected clones. The equal amounts of total proteins were subjected to SDS-PAGE with 7.5% gel. Bands of Cx43 were detected with the polyclonal rabbit anti-rat Cx43 antibody followed by the ECL. (B) Phosphorylation properties of wild-type Cx43 and Y265F mutant Cx43. Image of wild-type and Y265F mutant Cx43 on Western blot were captured by Image scanner and analyzed by NIH Image soft wear. Relative densities of bands of phosphorylated (P1 and P2) forms against nonphosphorylated (NP) form.

transfected with blank plasmid (A31-1-1/pB45) was also isolated. A31-1-1/pB45 cells were the same levels of Cx43 protein expression as those of A31-1-1 cells [Fig. 2(A)]. The level of phosphorylated Cx43 proteins in A31-1-1/Cx43Y265F cells partially declined compared with A31-1-1/Cx43 cells, because Y265F mutant Cx43 proteins are lacking in phosphorylation site of Tyr265 [Fig. 2(B)].

Enhancement of GJIC in A31-1-1/Cx43 and A31-1-1/Cx43Y265F cells

To assess functional GJIC, the SLDT assay was used. Lucifer yellow does not diffuse through intact plasma membranes, and its low molecular weight permits its transmission from one cell to another, presumably across patent gap junctions.[14–16] Therefore, the SLDT activities reflect the functional detection of GJIC. Levels of GJIC were evaluated with the SLDT method. Results of the experiments are shown in Figure 3. The level of GJIC of A31-1-1/Cx43 cells was 4.5 times as high as the A31-1-1 control cells. The level of GJIC of A31-1-1/Cx43Y265F cells was 3 times as high as A31-1-1 control cells. On the other hand, the level of GJIC of A31-1-1 cells transfected with control vector pB45-neo, A31-1-1/pB45 cells, was similar to A31-1-1 control cells.

Reduction of GJIC inhibition induced by MDU and PTMO1000

The actual distance of dye migration and GJIC inhibitory effects of MDU and PTMO1000 are showed in Figs. 4(A) and 5(A), respectively. In A31-1-1 control and A31-1-1/pB45 cells, GIJCs were inhibited by MDU (0.2 μg/mL) and PTMO1000 (2.0 μg/mL) down to 50% of vehicle (DMSO) control [Figs. 4(B) and 5(B)]. Although actual distance of dye migration in A31-1-1/Cx43 cells was much higher than A31-1-1 or A31-1-1/pB45 cells, GJIC inhibitory effects of MDU and PTMO1000 were the same level of A31-1-1 or A31-1-1/pB45 cells [Figs. 4(B) and 5(B)]. Though actual distance of dye migration in A31-1-1/Cx43Y265F cells was much higher than A31-1-1 or A31-1-1/pB45 cells, GJIC of A31-1-1/Cx43Y265F cells were not inhibited by MDU at all [Fig. 4(B)] and were partially inhibited by PTMO1000 [Fig. 5(B)]. These results indicate that

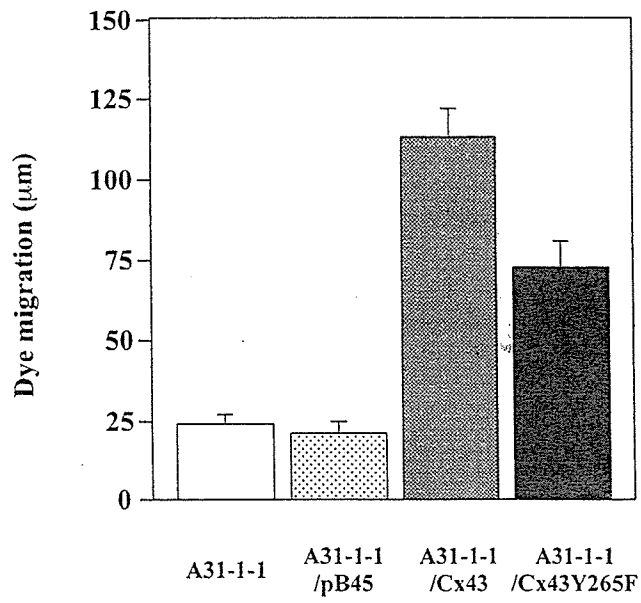

Figure 3. Gap junctional intercellular communication in A31-1-1, A31-1-1/pB45, A31-1-1/Cx43, and A31-1-1/Cx43Y265F cells measured by scrape loading and dye transfer (SLDT) method. Transmission of Lucifer yellow into contiguous cells detected 5 min after scrape-loading in A31-1-1, A31-1-1/pB45, A31-1-1/Cx43, and A31-1-1/Cx43Y265F cells.

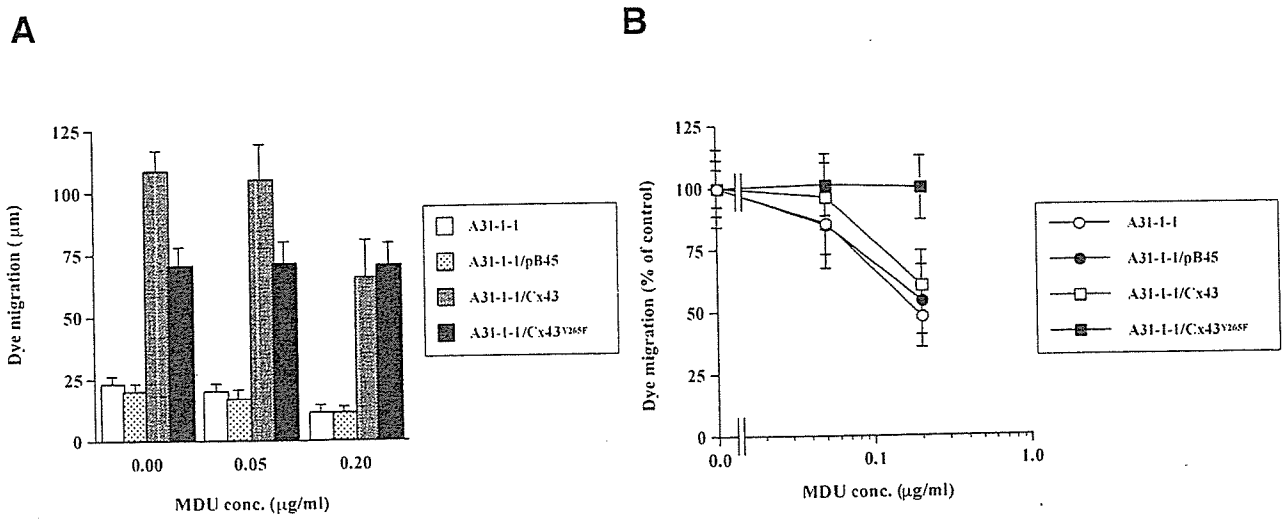

Figure 4. Inhibition of gap junctional intercellular communication by MDU. (A) Actual dye migration. (B) % of control.

Y265F mutant of Cx43 overcome the inhibitory effects by MDU and PTMO1000 probably through the avoidance from tyrosine phosphorylation of Tyr-265 on Cx43.

DISCUSSION

It has been known that many types of tumor cells suppressed Cx expression and inhibited GJIC. Many investigators had been reported that Cx gene transfection restored the tumorigenic phenotypes of such tumor cells.[17–22] To understand the mechanisms of tumorigenesis induced by biomaterials such as PEUs, polyethylene (PE), and poly-L-lactide (PLLA), we paid attention to the inhibitory effects on GJIC and examined its mechanisms. We hypothesized that the inhibition of GJIC in cells adhered to biomaterials bring about the enhancement of the cellular transformation. In our previous studies, we have shown that PEU, PE, and PLLA produced tumors in rat *in vivo*, and these biomaterials inhibited the GJIC *in vitro*.[6,7,9,23,24] In the present study, we established GJIC reinforced cells by transfected with Cx43 gene and examined the escaping effects from GJIC inhibition by biomaterials. We focused on the tumorigenic activity induced by PEUs, and PTMO1000 and MDU were used as model chemicals of PEU. PTMO1000 and MDU inhibited the GJIC in Balb/c 3T3 A31-1-1 cells.

Phosphorylation of Cx molecules closely related with the inhibition of GJIC.[25,26] Especially, phosphorylations of Tyr-265 on Cx43 molecule accelerate the binding to v-Src and inhibit the GJIC [Fig.6(A)].[27] Therefore, if the Tyr-265 of Cx43 was substituted with other amino acid such as phenylalanine (F), namely Y265F Cx43, Y256F Cx43 can not be phosphorylated at

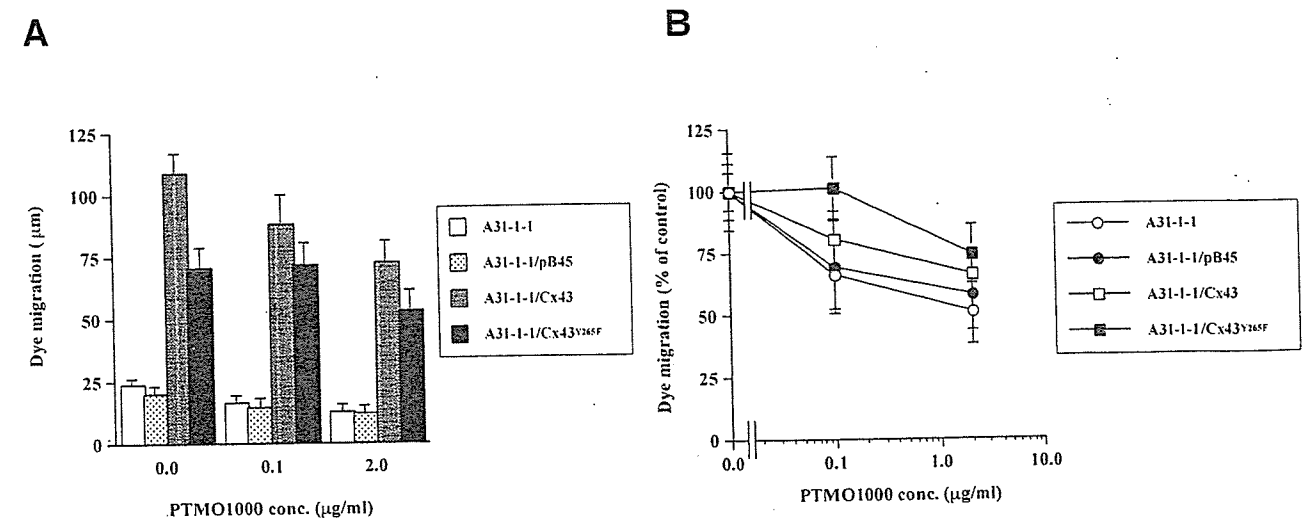

Figure 5. Inhibition of gap junctional intercellular communication by PTMO1000. (A) Actual dye migration. (B) % of control.

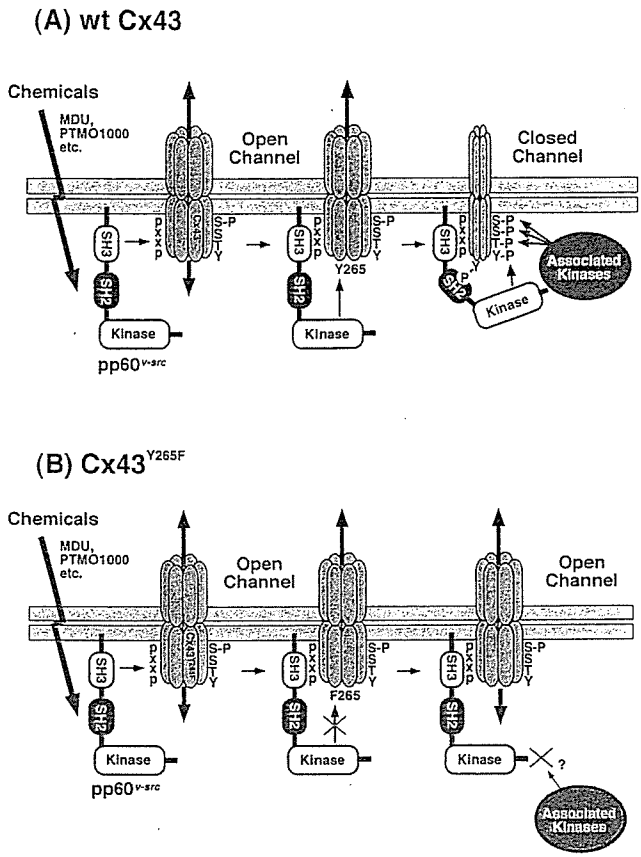

Figure 6. Model for escape from MDU and PTMO1000-induced GJIC inhibition in A31-1-1/Cx43Y265F cells. (A) The association between wild-type Cx43 and v-Src is initiated by the SH3 domain–proline-rich motif interaction, facilitating the phosphorylation of Cx43 on tyrosine 265 by v-Src. The association between Cx43 and v-Src is stabilized further by an SH2 domain–Tyr(P)-265 interaction, leading to additional phosphorylation of Cx43 by its own kinase domain or by v-Src-associated kinases. Hyperphosphorylation of Cx43 could lead to inhibition in GJIC function. (B) The association between Y265F mutant Cx43 and v-Src is also initiated by SH3 domain–proline-rich motif interaction. However, because the Tyr-265 phosphorylation site is substituted by Phe-265 on A31-1-1/Cx43Y265F cells, hyperphosphorylation of Cx43 does not occur and GJIC inhibition is abolished in this cell line. The "pxxp" is minimal consensus sequence for binding between Cx43 and pp60 v-src.[29,30]

the Phe-265(=F265) with tyrosine kinases such as v-Src as shown in Figure 6(B).

Therefore, transfection of Y265F Cx43 mutant fail to inhibition of GJIC induced by V-src kinase[28] because no phosphorylation was occurred at Phe-265 Cx43 [Fig. 6(B)].

There is a possibility that PTMO1000 and MDU inhibit the GJIC by the phosphorylation of Tyr-265 of Cx43. Therefore, we attempted that Y265F Cx43 mutant was transfected to A31-1-1 cells to prevent the inhibition of GJIC induced by PTMO1000 and MDU if both segments inhibit the GJIC by the enhancement of tyrosine kinases such as V-src kinase involving in the A31-1-1 cells. Overexpression of wild-type Cx43 led to great enhancement of GJIC, but remarkable improvement of the rate of inhibition of GJIC induced by PTMO and MDU was not observed. However, under the high concentrations of MDU and PTMO1000, which inhibit the GJIC in A31-1-1 and A31-1-1/pB45 cells, the level of GJIC in Cx43 overexpressed clone A31-1-1/Cx43 surpassed the parental (A31-1-1) and control (A31-1-1/pB45) cells. This result suggested that Cx43 transfection was effective for overcoming the inhibition of GJIC induced by MDU and PTMO1000. In A31-1-1/Cx43Y265F cells, the inhibitory effect on GJIC by MDU was completely disappeared, and the inhibitory effect of GJIC by PTMO1000 was partially recovered. These results suggest that the cause of inhibition of GJIC induced by MDU and PTMO1000 may be tyrosine phosphorylation of Tyr265 on Cx43 molecules in gap junctional cannels.

In the cells, there are possibilities that protein kinase C (PKC), which is a serine/threonine kinase, downregulates GJIC and the tyrosine kinase activities of the receptor for EGF and the Src oncoprotein are also inhibit the GJIC. We hypothesis that phosphorylation of tyrosine-265 of Cx43 may be a key step in the inhibitory effects on GJIC, and most potent candidate for tyrosine kinase involved in Tyr-265 phosphorylation of Cx43 is pp60 v-src. Kanemitsu et al.[27] demonstrated that pp60 v-sec direct phosphorylate Cx43 and inhibited the GJIC in v-src-transfirmed cells. Figure 6 summarizes a model that could account for the GJIC inhibition induced by MDU and PTMO1000 through pp60 v-src based on the model demonstrated by Kanemitsu et al.[27] Binding of v-Src to Cx43 is initiated by an SH3-mediated interaction, bringing the kinase domain of v-Src in close proximity to the Tyr-265 phosphorylation site of Cx43. After phosphorylation of Tyr-265 by v-Src, the association is stabilized by an SH2-Tyr(P)-265 interaction. Cx43 may be further phosphorylated on other tyrosines by v-Src, or on serines by v-Src-associated kinases. Hyperphosphorylation of Cx43 results in GJIC inhibition. On the other hand, because Y265F Cx43 do not have Tyr-265 phosphorylated site by v-Src, hyperphosphorylation of Cx43 is not caused. Therefore, GJIC is not inhibited by MDU and PTMO1000.

In conclusion, we established the cell lines expressing wild-type Cx43 or Y265F mutant Cx43 to prevent the inhibition of GJIC induced by biomaterials, such as PEU. These cell lines were maintained with much higher GJIC levels than the control cells even under the existence of the hard and soft segments of PEU. Especially, the Cx43 Y265F mutant prevents the inhibition of GJIC induced by MDU, PEU hard segment.

The authors thank Dr. David L. Paul (Department of Neurobiology, Harvard Medical School) and Dr. Eckhard R. Podack (Department of Microbiology, University of Miami) for

kindly providing rat Cx43 cDNA and pB45-neo plasmid vector, respectively.

References

1. Goodenough DA, Goliger JA, Paul DL. Connexins, connexons, and intercellular communication. Annu Rev Biochem 1996;65: 475–502.
2. Kumar NM, Gilula NB. The gap junction communication channel. Cell 1996;84:381–388.
3. Wu Y, Selliti C, Anderson JM, Hiltner A, Lodoen GA, Payet CR. An FTIR-ATR investigation of in vivo by poly (etherurethane) degradation. J Appl Polym Sci 1992;46:201–211.
4. Xi T, Sato M, Nakamura A, Kawasaki Y, Umemura T, Tsuda M, Kurokawa Y. Degradation of polyetherurethane by subcutaneous implantation in rats. I. Molecular weight change and surface morphology. J Biomed Mater Res 1994;28:483–490.
5. Nakamura A, Kawasaki Y, Takada K, Aida Y, Kurokawa Y, Kojima S, Shintani H, Matsui M, Nohmi T, Matsuoka A, Sofuni T, Kurihara M, Miyata N. Difference in tumor incidence and other tissue responses to polyetherurethanes and polydimethylsiloxane in long-term subcutaneous implantation into rats. J Biomed Mater Res 1992;26:631–650.
6. Tsuchiya T, Hata H, Nakamura A. Studies on the tumor promoting activity of biomaterials: Inhibition of metabolic cooperation by polyetherurethane and silicone. J Biomed Mater Res 1995;29:113–119.
7. Tsuchiya T, Takahara A, Cooper SL, Nakamura A. Studies on the tumor promoting activity of polyurethanes: Depletion of inhibitory action of the metabolic cooperation on the surface of a polyalkyleneurethane but not a polyetherurethane. J Biomed Mater Res 1995;29:835–841.
8. Tsuchiya T, Nakaoka R, Degawa H, Nakamura A. Studies on the mechanisms of tumorigenesis induced by polyetherurethanes in rats: Leachable and biodegradable oligomers involving the diphenyl carbamate structure acted as an initiator on the transformation of Balb 3T3 cells. J Biomed Mater Res 1996;31:299–303.
9. Tsuchiya T, Nakamura A. Effect of different implant materials on inhibition of gap-junctional intercellular communication as an index of tumor promotion. IARC monographs on the evaluation of carcinogenic risks to humans. Surgical Implants Other and Foreign Bodies 1999;74:290–293.
10. Tsuchiya T, Nakamura A. What initiates the formation of preneoplastic parent cells? IARC monographs on the evaluation of carcinogenic risks to human. Surgical Implants Other Foreign Bodies 1999;74:293–294.
11. Karasuyama H, Melchers F. Establishment of mouse cell lines which constitutively secrete large quantities of interleukin 2, 3, 4 or 5, using modified cDNA expression vectors. Eur J Immunol 1988;18:97–104.
12. El-Fouly MH, Trosko JE, Chang CC. Scrape-loading and dye transfer: Arapid and simple technique to study gap junctional intercellular communication. Exp Cell Res 1987;168:422–430.
13. Upham BL, Yao JJ, Trosko JE, Masten SJ. Determination of the efficacy of ozone treatment systems using a gap junction intercellular communication bioassay. Environ Sci Technol 1995;29: 2923–2928.
14. Stewart WW. Functional connections between cells as revealed by dye-coupling with a highly fluorescent naphthalimide tracer. Cell 1978;14:741–759.
15. Stewart WW. Lucifer dye—highly fluorescent dyes for biological tracing. Nature 1981;292:17–21.
16. Lo CW, Gilula NB. Gap junctional communication in the postimplantation mouse embryo. Cell 1979;18:411–422.
17. Huang RP, Fan Y, Hossain MZ, Peng A, Zeng ZL, Boynton AL. Reversion of the neoplastic phenotype of human glioblastoma cells by connexin 43 (cx43). Cancer Res 1998;58:5089–5096.
18. Zhang ZQ, Zhang W, Wang NQ, Bani-Yaghoub M, Lin ZX, Naus CC. Suppression of tumorigenicity of human lung carcinoma cells after transfection with connexin43. Carcinogenesis 1998;19:1889–1894.
19. Eghbali B, Kessler JA, Reid LM, Roy C, Spray DC. Involvement of gap junctions in tumorigenesis: transfection of tumor cells with connexin 32 cDNA retards growth in vivo. Proc Natl Acad Sci USA 1991;88:10701–10705.
20. Zhu D, Caveney S, Kidder GM, Naus CC. Transfection of C6 glioma cells with connexin 43 cDNA: analysis of expression, intercellular coupling, and cell proliferation. Proc Natl Acad Sci USA 1991;88:1883–1887.
21. Naus CC, Elisevich K, Zhu D, Belliveau DJ, Del Maestro RF. In vitro growth of C6 glioma cells transfected with connexin 43 cDNA. Cancer Res 1992;52:4208–4213.
22. Mesnil M, Krutovskikh V, Piccoli C, Elfgang C, Traub O, Willecke K, Yamasaki H. Negative growth control of HeLa cells by connexin genes: connexin species specificity. Cancer Res 1995; 55:629–639.
23. Tsuchiya T. A useful marker for evaluating the tissue engineering products: gap junctional communication for assessment of the tumor-promoting action and disruption of cell differentiation in the tissue engineering products. J Biomater Sci Polym Ed 2000;11:947–959.
24. Nakaoka R, Tsuchiya T, Kato K, Ikada Y, Nakamura A. Studies on tumor-promotion activity of polyethylene: inhibitory activity of metabolic cooperation on polyethylene surfaces is markedly decreased by surface modification with collagen but not with RGDS peptide. J Biomed Mater Res 1997;35:391–397.
25. Musil LS, Cunningham BA, Edelman GM, Goodenough DA. Differential phosphorylation of the gap junction protein connexin43 in junctional communication-competent and -deficient cell lines. J Cell Biol 1990;111:2077–2088.
26. Lampe PD, Lau AF. Regulation of gap junctions by phosphorylation of connexins. Arch Biochem Biophys 2000;384:205–215.
27. Kanemitsu MY, Loo LW, Simon S, Lau AF, Eckhart W. Tyrosine phosphorylation of connexin 43 by v-Src is mediated by SH2 and SH3 domain interactions. J Biol Chem 1997;272:22824–22831.
28. Swenson KI, Piwnica-Worms H, McNamee H, Paul DL. Tyrosine phosphorylation of the gap junction protein connexin43 is required for the pp60v-src-induced inhibition of communication. Cell Regul 1990;1:989–1002.
29. Rickles RJ, Botfield MC, Weng Z, Taylor JA, Green OM, Brugge JS, Zoller MJ. Identification of Src, Fyn, Lyn, PI3K and Abl SH3 domain ligands using phage display libraries. EMBO J 1994; 13:5598–5604.
30. Rickles RJ, Botfield MC, Zhou XM, Henry PA, Brugge JS, Zoller MJ. Phage display selection of ligand residues important for Src homology 3 domain binding specificity. Proc Natl Acad Sci USA 1995;92:10909–10913.

J. Biomater. Sci. Polymer Edn, Vol. 13, No. 2, pp. 153–166 (2002)

Effect of γ-ray irradiated poly(L-lactide) on the differentiation of mouse osteoblast-like MC3T3-E1 cells

K. ISAMA * and T. TSUCHIYA

Division of Medical Devices, National Institute of Health Sciences, Kamiyoga 1-18-1, Setagaya-ku, Tokyo 158-8501, Japan

Received 18 June 2001; accepted 10 December 2001

Abstract—The purpose of this study was to clarify the effects of γ-ray irradiated poly(L-lactide) (PLLA) on the proliferation and differentiation of mouse osteoblast-like MC3T3-E1 cells. The PLLA was γ-irradiated at the dose of 10, 25 or 50 kGy, and the molecular weight of irradiated PLLA decreased with increasing irradiation dose. The proliferation and differentiation of MC3T3-E1 cells cultured on irradiated PLLA for 2 weeks were evaluated using micromass culture. The γ-irradiation of PLLA did not affect the proliferation, but stimulated the differentiation of MC3T3-E1 cells cultured on irradiated PLLA. These results suggested that lower change in the molecular weight of PLLA was responsible for stimulation of the differentiation of MC3T3-E1 cells cultured on irradiated PLLA. Furthermore, the proliferation and calcification of MC3T3-E1 cells cultured in the medium containing low molecular weight PLLA for 2 weeks were evaluated. The low molecular weight PLLA also stimulated the calcification of MC3T3-E1 cells with no effect on the proliferation. The γ-irradiation was suitable for PLLA on the differentiation of mouse osteoblasts.

Key words: Poly(L-lactide); γ-ray irradiation; osteoblast; MC3T3-E1 cells; differentiation.

INTRODUCTION

Poly(L-lactide) (PLLA) is a biodegradable material used in medical and pharmaceutical applications. There have been many reports on the bioabsorbability and biocompatibility of PLLA. Bos *et al.* reported that the mass loss of PLLA was observed after 26 weeks and no acute or chronic inflammatory reaction to PLLA was observed until 143 weeks by subcutaneous implantation into rats [1]. Otto *et al.* observed lamellar bone formation around the PLLA wire at 2 and 6 months after intramedullary implantation into rat tibiae [2]. Mainil-Varlet *et al.* also observed decreasing molecular weight of PLLA after 4 weeks and bone formation around the PLLA pin at 1 month after implantation into the cortex of sheep tibiae [3]. Thus,

*To whom correspondence should be addressed. E-mail: isama@nihs.go.jp

the high molecular weight PLLA has been used as biodegradable screws, pins and plates for internal bone fixation in orthopedics.

Sterilization is essential for implant medical devices. Ethylene oxide sterilization was reported to have a risk of carcinogenicity because of the mutagenic properties of ethylene oxide [4]. On the other hand, autoclave sterilization causes plastic deformation and extensive hydrolytic degradation, and dry heat sterilization leads to thermo-oxidative degradation of the material [5]. Ikarashi *et al.* reported that the molecular weight of PLLA was decreased and the activity of MC3T3-E1 cells cultured on PLLA was enhanced by heat treatment of PLLA [6]. γ-Ray irradiation has been known as an alternative method for sterilizing the material when other sterilization methods are not suitable. However, it is known that γ-irradiation causes polymer chain scission. Yoshioka *et al.* observed that the molecular weight of poly(DL-lactide) (PDLLA) decreased and the carboxylic acid content increased with increasing irradiation dose [7, 8]. Zhang *et al.* reported that γ-irradiation accelerated the hydrolytic degradation of poly(glycolide-lactide) copolymer and poly(glycolide-trimethylene carbonate) sutures *in vitro*, and the former was more sensitive to γ-irradiation than the latter [9]. Slivka *et al.* also observed that γ-irradiation of calcium phosphate/PLLA composite accelerated the rate of interface degradation *in vitro* [10]. Thus, γ-irradiation may change the physicochemical properties of PLLA, but there is no detailed information on the relation between γ-irradiated PLLA and osteoblast function.

The purpose of this study was to clarify the effects of γ-ray irradiated PLLA on the proliferation and differentiation of osteoblasts. The change in molecular weight with γ-irradiation of PLLA was shown. Mouse osteoblast-like MC3T3-E1 cells were cultured on irradiated PLLA, and then the proliferation and calcification of MC3T3-E1 cells were evaluated using the micromass culture. The biological activities of MC3T3-E1 cells cultured on irradiated PLLA were measured. We also examined the effects of low molecular weight PLLA on the proliferation and calcification of MC3T3-E1 cells.

MATERIALS AND METHODS

Materials

PLLA sheets made of high molecular weight PLLA with thickness of 0.3 mm were obtained from Shimadzu Co. (Kyoto, Japan). PLLA with weight average molecular weight of 5000 (PLLA 5000) and 10 000 (PLLA 10 000) were obtained from Nacalai Tesque, Inc. (Kyoto, Japan).

γ-Ray irradiation of PLLA

The PLLA sheets were γ-ray irradiated at the dose of 10, 25 or 50 kGy using ^{60}Co as the radiation source. The irradiated PLLA sheets were preserved in a silica gel

desiccator until the next experiment. The PLLA sheets were cut into 14.0 mm diameter disks and sterilized both sides with ultraviolet rays for 15 h, respectively. It was confirmed that there was no change in Fourier transform infrared attenuated total reflection (FT-IR/ATR) spectroscopy by ultraviolet irradiation for the PLLA disks.

Gel permeation chromatography

The molecular weight of PLLA was determined by gel permeation chromatography (GPC). The LC10AT (Shimadzu Co., Kyoto, Japan) equipped with refractive index detector (RID-10A, Shimadzu Co.) was used as a GPC apparatus. PLLA samples were dissolved in chloroform at a concentration of 5 mg/ml. Fifty microliters of sample solution were eluted through two GPC columns (TSKgel $G5000H_{XL}$ + TSKgel $G4000H_{XL}$, each 7.8 mm i.d. × 300 mm, Tosoh, Tokyo, Japan) at a mobile phase of 1.0 ml/min chloroform. The weight average molecular weight (M_w) and number average molecular weight (M_n) of PLLA were analyzed from the comparison with the calibration curve that was made with polystyrene standards (Showa Denko, Tokyo, Japan) using LC workstation, CLASS-LC 10 (Shimadzu Co.).

Micromass culture

Mouse osteoblast-like MC3T3-E1 cells were obtained from RIKEN Cell Bank (Saitama, Japan), and were grown in alpha minimum essential medium (α-MEM) (Gibco Laboratories, Grand Island, New York) supplemented with 20% fetal bovine serum (Intergen, Purchase, New York), 100 μg/ml penicillin and 100 mU/ml streptomycin in a 37°C humidified atmosphere of 5% CO_2. The cells were passaged with 0.05% trypsin and 0.1% ethylenediaminetetraacetic acid tetrasodium salt solution (Gibco Laboratories).

The γ-ray irradiated PLLA disks were laid in the well of type I collagen coated 24-well dish (Iwaki Glass, Tokyo, Japan). Cell suspensions were prepared in the culture medium and adjusted to give 2×10^6 cells/ml. A 20 μl aliquot of the cell suspensions was delivered to each well of type I collagen coated 24-well dish or on the γ-irradiated PLLA disk which was laid in the well of the 24-well dish. After the cells were attached on the PLLA disk, 1 ml of the complete medium that contained 10 mM disodium β-glycerophosphate (β-GP) (Sigma Chemical Co., St. Louis, Missouri) in the culture medium was added. The complete medium was changed three times a week, and the cells were cultured for 2 weeks.

The effects of low molecular weight PLLA on the proliferation and calcification of MC3T3-E1 cells were investigated as fellows: PLLA 5000 and PLLA 10 000 were dissolved in dimethyl sulfoxide (DMSO) to a concentration of 50 mg/ml, respectively, and sterilized by filtration through a 0.22 μm filter. The PLLA solution was diluted by the complete medium at 1000 times. After the spot-like cells were attached on the well of type I collagen coated 24-well dish, 1 ml of the complete

medium containing low molecular weight PLLA, or an equal amount (1 μl) of DMSO as a vehicle control, was added. The complete medium containing each chemical at the same concentration was changed three times a week, and the cells were cultured for 2 weeks.

Experiments were performed at least two times.

Proliferation assay

The proliferation of MC3T3-E1 cells was determined by using cell proliferation assay reagent, TetraColor ONE (Seikagaku Co., Tokyo, Japan). The cell cultures were exchanged with the culture medium containing 2% TetraColor ONE, and were incubated for 2 h. The absorbance of the medium was read at 450 nm (reference at 600 nm). It has been proven that the absorbance and cell population show a linear relationship.

Calcification assay

After the proliferation was determined, the cell cultures were washed three times with Dulbecco's phosphate-buffered saline without calcium and magnesium salts (PBS(−)) and fixed by the addition of 10% formalin dissolved in PBS(−) solution. After fixing, the cultures were washed five times with water and stained by alizarin red S solution. The transmission digital images of alizarin red S stained cultures were obtained with a color image scanner (GT-9500WIN, SEIKO EPSON Co., Nagano, Japan) with transparency unit (GT95FLU, SEIKO EPSON Co.), and then, the alizarin red S stained areas were measured using an image processing and analysis software, Scion Image (Scion Co., Frederick, Maryland).

Preparation of cell lysates

Protein, DNA, hydroxyproline (HYP) contents and alkaline phosphatase (ALP) activity of MC3T3-E1 cells cultured on γ-ray irradiated PLLA for 2 weeks were measured using the cell lysates prepared according to the method described below [11]: The cell cultures were washed twice with PBS(−). The cells were recovered by trypsinization and washed twice with PBS(−) by centrifugation at 1000 rpm for 2 min. The residues were resuspended in 1 ml of 0.2% Nonidet P-40 solution and sonicated in an ice bath for 2 min using ultrasonic processor (VC-50T, Sonic & Materials Inc., Danbury, Connecticut). The cell lysates were stored frozen at −20°C until measurement.

Protein content

Protein content of cell lysates was measured by the method of Lowry *et al.* [12] with minor modification. The alkaline copper solution was freshly made: Fifty milliliters of 0.1 N NaOH containing 2% Na_2CO_3 was mixed with 1 ml of 0.5%